Microarrays Assembled in Microfluidic Chips Fabricated from Poly(methyl methacrylate) for the Detection of Low-Abundant DNA Mutations

ARTICLE *in* ANALYTICAL CHEMISTRY · MARCH 2003

Impact Factor: 5.64 · DOI: 10.1021/ac020683w · Source: PubMed

Anal. Chem. **2003,** *75,* 1130−1140

Microarrays Assembled in Microfluidic Chips Fabricated from Poly(methyl methacrylate) for the Detection of Low-Abundant DNA Mutations

Yun Wang, Bikas Vaidya, Hannah D. Farquar, Wieslaw Stryjewski, Robert P. Hammer, Robin L. McCarley, and Steven A. Soper*

Department of Chemistry, Louisiana State University, Baton Rouge, Louisiana 70803-1804

Yu-Wei Cheng and Francis Barany

Department of Microbiology, Joan and Sanford I. Weill Medical College of Cornell University, New York, New York 10021

Low-density arrays were assembled into microfluidic channels hot-embossed in poly(methyl methacrylate) (PMMA) to allow the detection of low-abundant mutations in gene fragments (*K-ras*) that carry point mutations with high diagnostic value for colorectal cancers. Following spotting, the chip was assembled with a cover plate and the array accessed using microfluidics in order to enhance the kinetics associated with hybridization. The array was configured with zip code sequences (24-mers) that were complementary to sequences present on the target. The hybridization targets were generated using an allele-specific ligase detection reaction (LDR), in which two primers (discriminating primer that carriers the complement base to the mutation being interrogated and a common primer) that flank the point mutation and were ligated (joined together) only when the particular mutation was present in the genomic DNA. The discriminating primer contained on its 5′-end the zip code complement (directs the LDR product to the appropriate site of the array), and the common primer carried on its 3′ end a fluorescent dye (near-IR dye IRD-800). The coupling chemistry (5′-amine-containing oligonucleotide tethered to PMMA surface) was optimized to maximize the loading level of the zip code oligonucleotide, improve hybridization sensitivity (detection of low-abundant mutant DNAs in high copy numbers of normal sequences), and increase the stability of the linkage chemistry to permit re-interrogation of the array. It was found that microfluidic addressing of the array reduced the hybridization time from 3 h for a conventional array to less than 1 min. In addition, the coupling chemistry allowed reuse of the array >12 times before noticing significant loss of hybridization signal. The array was used to detect a point mutation in a *K-ras* oncogene at a level of 1 mutant DNA in 10 000 wild-type sequences.

With completion of the first rough draft of the human genome, new genes are being discovered at an accelerated rate as well as the function of these genes (functional genomics). In addition, the association of certain genes or mutations within these genes with particular phenotypes (disease states) has produced an array of new diagnostic markers for predicting or monitoring the course of treatments for genetic-based diseases. Indeed, many diseases have already been determined to possess genetic links. Sickle cell anemia has been linked to a single base mutation in the β-globin gene (substitution of an adenosine in the wild type with a thymosine at the second position of the sixth codon of the β gene in the mutated form).[1] Many diseases have also been found to carry several different mutations in different genes, all of which can and sometimes must be used for the accurate diagnosis of that phenotype. For example, colorectal adenomas and cancers have been determined to possess point mutations in *K-ras* genes (19 different point mutations), which can occur early in the development of the disease in nearly 30−50% of patients.[2−6]

There are several analytical challenges associated with detecting genetic mutations for diagnostics: (1) The mutation may be a single-base polymorphism isolated on a single gene fragment. With appropriately designed PCR primers that flank the mutation site, the gene fragment containing the mutation can be readily amplified and then analyzed for its allelic composition using several different techniques including allele-specific hybridization, allele-specific PCR, or various electrophoretic methods (denaturant gradient gel electrophoresis, single-strand conformational polymorphism, etc.). (2) Many disease states require the monitoring of several different mutations, which can be single-base mutations,

* To whom correspondence should be addressed. E-mail: steve.soper@chemgate.chem.lsu.edu.

(1) Pauling, L.; Itano, H. A.; Singer, S. J.; Wells, I. C. *Science* **1949**, *110*, 543−548.
(2) Rothschild, C. B.; Brewer, C. S.; Loggie, B.; Beard, G. A.; Triscott, M. X. *J. Immunol. Methods* **1997**, *206*, 11−19.
(3) Otori, K.; Oda, Y.; Sugiyama, K.; Hasebe, T.; Mukai, K.; Fujii, T.; Tajiri, H.; Yoshida, S.; Fukushima, S.; Esumi, H. *Gut* **1997**, *40*, 660−663.
(4) Mulcahy, H. E.; Anker, P.; Chen, X.; Lefort, F.; Vasioukhin, V.; Lyautey, J.; Lederrey, C.; Stroun, M.; Farthing, M. J. G. *Gastroenterology* **1996**, *110*, A563−A563.
(5) Chiang, J. M. *Cancer Lett.* **1998**, *126*, 179−185.
(6) Andersen, S. N.; Lovig, T.; Breivik, J.; Lund, E.; Gaudernack, G.; Meling, G. I.; Rognum, T. O. *Scand. J. Gastroenterol.* **1997**, *32*, 62−69.

10.1021/ac020683w CCC: $25.00
Published on Web 01/24/2003

repeat expansions, deletions, or frame shifts that can occur on several different gene fragments. For example, colorectal cancers manifest themselves as genetic alterations that occur not only in *K-ras* genes but others as well such as APC, p53, and BAX genes.[7−14] In these cases, multiplexed assays are required, in which all of the mutations are screened simultaneously in order to obtain a clear picture of the phenotypic state of the patient. (3) The mutation of interest (mutant DNA) may be present in low copy number (minority) in a mixed population of higher copy number wild-type or normal DNA. Even at the primary tumor site for many cancers, the normal stromal cell content can be as high as 70%. Therefore, if the mutation is found in only one of the two chromosomes of a tumor cell (heterozygous), the mutated DNA can be present in as little as 15% of the DNA found in a sample containing the target gene.[15] This number goes down precipitously if the sampling is done away from the primary tumor site.

To detect low-abundant mutations for diagnostics it becomes necessary to include a step into the assay that can distinguish with high sensitivity wild-type from mutant DNA. One such technique is the ligase detection reaction (LDR) coupled to a primary PCR reaction.[16−25] A diagram of the PCR/LDR technique is depicted in Figure 1. Following PCR amplification of the appropriate gene fragment, which contains a section of the gene that possesses the point mutations, the amplicon is mixed with two LDR primers that flank the mutation of interest (common primer and discriminating primer). The discriminating primer contains a base at its 3′ end that coincides with the single-base mutation site. If there is a mismatch, ligation of the two primers does not occur. However, a perfect match results in the successful ligation of the two primers and produces a product that can be analyzed in a variety of fashions. The advantages of the PCR/LDR assay are that it can be configured to do highly multiplexed assays, uses a thermally stable ligase enzyme (*Tth* ligase) to linearly amplify the LDR product to aid in detection, and can potentially detect 1 mutant DNA in >1000 copies of normal DNA.

DNA microarrays can be configured to detect sequence variations at many different sites simultaneously and, as such, can be used for diagnostic applications.[26−38] These arrays consist of thousands of short oligonucleotide probes (∼20-mers) with known sequence attached covalently or noncovalently to two-dimensional solid surfaces such as glass via siloxane chemistry or electrostatically to polylysine-coated slides.[39] Some of the limitations associated with microarrays include the extended hybridization times required to elicit an optimal response (diffusion-controlled passive hybridization), the instability of the linkage chemistry (hydrolytically unstable), and the large amount of sample required to interrogate the array. The use of microarrays for detecting single-nucleotide variations typically involves the hybridization of labeled targets to surface-tethered probes[40−42] or polymerase extension of arrayed primers.[43,44] Due to the similarities in the hybridization thermodynamics (single-base mismatched versus fully matched duplexed DNA with the mutant DNA being a minority) ambiguities result, making it difficult to detect low-abundant point mutations using allele-specific probes in an array format.

Recently, universal zip code arrays have been developed for screening many single-base mutations in low abundance and can be used as a universal platform for molecular recognition.[15,45,46] The array format (see Figure 1) uses small probes that serve as

(7) Fearon, E. R.; Vogelstein, B. *Cell* **1990**, *61*, 759−767.
(8) Bronner, C. E.; Baker, S. M.; Morrison, P. T.; Warren, G.; Smith, L. G.; Lescoe, M. K.; Kane, M.; Earabino, C.; Lipford, J.; Lindblom, A.; Tannergard, P.; Bollag, R. J.; Godwin, A. R.; Ward, D. C.; Nordenskjold, M.; Fishel, R.; Kolodner, R.; Liskay, R. M. *Nature* **1994**, *368*, 258−261.
(9) Fishel, R.; Lescoe, M. K.; Rao, M. R. S.; Copeland, N. G.; Jenkins, N. A.; Garber, J.; Kane, M.; Kolodner, R. *Cell* **1993**, *75*, 1027−1038.
(10) Korinek, V.; Barker, N.; Morin, P. J.; vanWichen, D.; deWeger, R.; Kinzler, K. W.; Vogelstein, B.; Clevers, H. *Science* **1997**, *275*, 1784−1787.
(11) Leach, F. S.; Nicolaides, N. C.; Papadopoulos, N.; Liu, B.; Jen, J.; Parsons, R.; Peltomaki, P.; Sistonen, P.; Aaltonen, L. A.; Nystromlahti, M.; Guan, X. Y.; Zhang, J.; Meltzer, P. S.; Yu, J. W.; Kao, F. T.; Chen, D. J.; Cerosaletti, K. M.; Fournier, R. E. K.; Todd, S.; Lewis, T.; Leach, R. J.; Naylor, S. L.; Weissenbach, J.; Mecklin, J. P.; Jarvinen, H.; Petersen, G. M.; Hamilton, S. R.; Green, J.; Jass, J.; Watson, P.; Lynch, H. T.; Trent, J. M.; Delachapelle, A.; Kinzler, K. W.; Vogelstein, B. *Cell* **1993**, *75*, 1215−1225.
(12) Morin, P. J.; Sparks, A. B.; Korinek, V.; Barker, N.; Clevers, H.; Vogelstein, B.; Kinzler, K. W. *Science* **1997**, *275*, 1787−1790.
(13) Papadopoulos, N.; Nicolaides, N. C.; Wei, Y. F.; Ruben, S. M.; Carter, K. C.; Rosen, C. A.; Haseltine, W. A.; Fleischmann, R. D.; Fraser, C. M.; Adams, M. D.; Venter, J. C.; Hamilton, S. R.; Petersen, G. M.; Watson, P.; Lynch, H. T.; Peltomaki, P.; Mecklin, J. P.; Delachapelle, A.; Kinzler, K. W.; Vogelstein, B. *Science* **1994**, *263*, 1625−1629.
(14) Rampino, N.; Yamamoto, H.; Ionov, Y.; Li, Y.; Sawai, H.; Reed, J. C.; Perucho, M. *Science* **1997**, *275*, 967−969.
(15) Gerry, N. P.; Witowski, N. E.; Day, J.; Hammer, R. P.; Barany, G.; Barany, F. *J. Mol. Biol.* **1999**, *292*, 251−262.
(16) Barany, F. *Proc. Natl. Acad. Sci. U.S.A.* **1991**, *88*, 189−193..
(17) Wei, Q.; Barany, F.; Wilson, V. L. *Mol. Biol. Cell* **1992**, *3*, A22-A22.
(18) Wiedmann, M.; Barany, F.; Batt, C. A. *Appl. Environ. Microbiol.* **1993**, *59*, 2743−2745.
(19) Wiedmann, M.; Wilson, W. J.; Czajka, J.; Luo, J. Y.; Barany, F.; Batt, C. A. *Pcr-Methods Appl.* **1994**, *3*, S51−S64.
(20) Day, D. J.; Speiser, P. W.; White, P. C.; Barany, F. *Genomics* **1995**, *29*, 152−162.
(21) Luo, J. Y.; Bergstrom, D. E.; Barany, F. *Nucleic Acids Res.* **1996**, *24*, 3071−3078.
(22) Luo, J. Y.; Barany, F. *Nucleic Acids Res.* **1996**, *24*, 3079−3085.
(23) Khanna, M.; Cao, W. G.; Zirvi, M.; Paty, P.; Barany, F. *Clin. Biochem.* **1993**, *32*, 287−290.
(24) Khanna, M.; Park, P.; Zirvi, M.; Cao, W. G.; Picon, A.; Day, J.; Paty, P.; Barany, F. *Oncogene* **1999**, *18*, 27−38.
(25) Tong, J.; Cao, W. G.; Barany, F. *Nucleic Acids Res.* **1999**, *27*, 788−794.
(26) Consolandi, C.; Castiglioni, B.; Bordoni, R.; Busti, E.; Battaglia, C.; De Bellis, G. *Minerva Biotecnol.* **2001**, *13*, 261−268.
(27) De Benedetti, V. M. G.; Biglia, N.; Sismondi, P.; De Bortoli, M. *Int J. Biol. Markers* **2000**, *15*, 1−9.
(28) Dimitrjevic, B. *Jugosl. Med. Biohem.* **2001**, *20*, 65−71.
(29) Gregg, J. *Clin. Chem.* **1999**, *45*, S13−S13.
(30) Gupta, P. K.; Roy, J. K.; Prasad, M. *Curr. Sci.* **1999**, *77*, 875−884.
(31) Hacia, J. G.; Collins, F. S. *J. Med. Genet.* **1999**, *36*, 730−736.
(32) Hacia, J. G. *Nat. Genet.* **1999**, *21*, 42−47.
(33) Haviv, I.; Campbell, I. G. *Mol. Cell. Endocrino.* **2002**, *191*, 121−126.
(34) Kolchinsky, A.; Mirzabekov, A. *Hum. Mutat.* **2002**, *19*, 343−360.
(35) Lee, P.; Hudson, T. J. *M S-Med. Sci.* **2000**, *16*, 43−49.
(36) Petrik, J. *Vox Sang.* **2001**, *80*, 1−11.
(37) Tawata, M.; Aida, K.; Onaya, T. *Comb. Chem. High Throughput Screening* **2000**, *3*, 1−9.
(38) Zakhrabekova, S.; Kannangara, C. G.; von Wettstein, D.; Hansson, M. *Plant Physiol. Biochem.* **2002**, *40*, 189−197.
(39) Southern, E.; Mir, K.; Shchepinov, M. *Nat. Genet.* **1999**, *21*, 5−9.
(40) Beattie, K. L.; Beattie, W. G.; Meng, L.; Turner, S. L.; Coral-Vazquez, R.; Smith, D. D.; McIntyre, P. M.; Dao, D. D. *Clin. Chem.* **1995**, *41*, 700−706.
(41) Guo, Z.; Liu, Q.; Smith, L. M. *Nucleic Acids Res.* **1994**, *22*, 5456−5465.
(42) Hacia, J. G.; Brody, L. C.; Chee, M. S.; Fodor, S. P.; Collins, F. S. *Nat. Genet.* **1996**, *14*, 441−447.
(43) Nikiforov, T. T.; Rendle, R. B.; Goelet, P.; Rogers, Y. H.; Kotewicz, M. L.; Anderson, S.; Trainor, G. L.; Knapp, M. R. *Nucleic Acids Res.* **1994**, *22*, 4167−4175.
(44) Lockley, A. K.; Jones, C. G.; Bruce, J. S.; Franklin, S. J.; Bardsley, R. G. *Nucleic Acids Res.* **1997**, *25*, 1313−1314.
(45) Favis, R.; Barany, F. In *Circulating Nucleic Acids in Plasma or Serum*; Anker, P., Stroun, M., Eds.; Annuals of the New York Academy of Sciences 906; New York Academy of Sciences: New York, 2000; pp 39−43.
(46) Favis, R.; Day, J. P.; Gerry, N. P.; Phelan, C.; Narod, S.; Barany, F. *Nat. Biotechnol.* **2000**, *18*, 561−564.

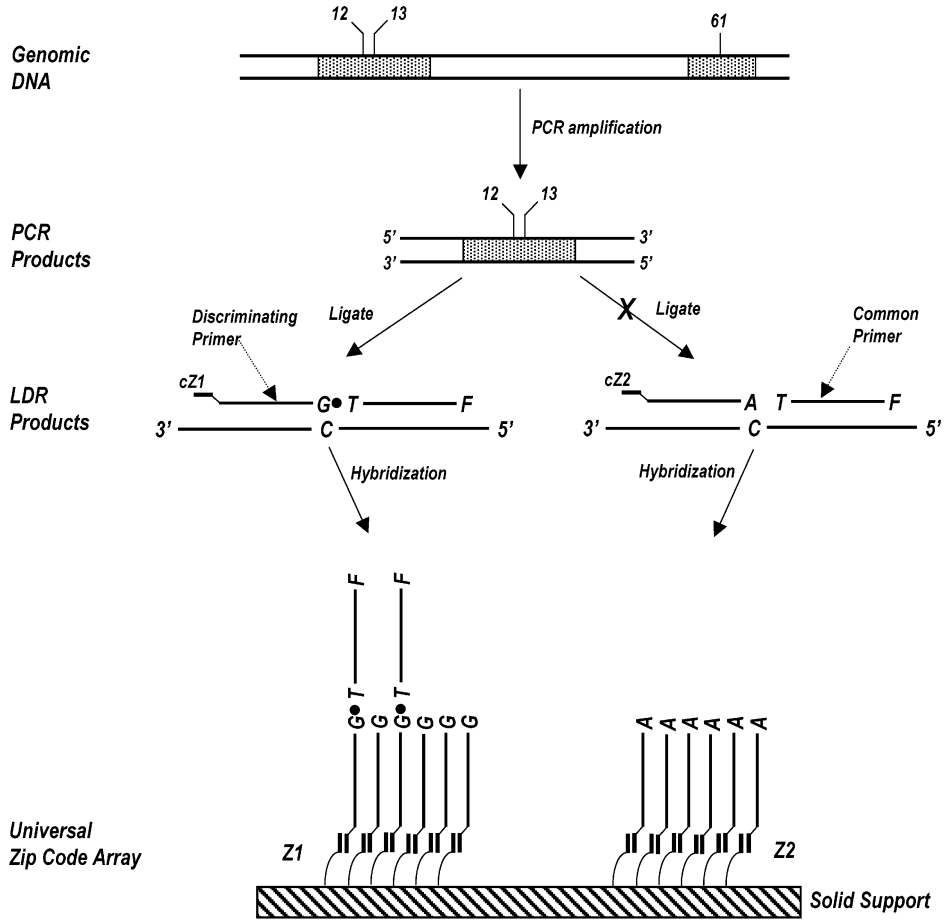

Figure 1. Schematic showing the LDR process and hybridization to zip code oligonucleotide probes arrayed on a solid substrate.

zip codes (24-mers with similar T_m values) and contain unique sequences not found in the test DNA template. The PCR/LDR uses discriminating and common primers similar to that described above. However, the allele-specific primer contains on its 5′-end a zip code complement that directs the ligation product to a particular site of the array. The common primer contains a fluorescent dye on its 3′ end. If the mutation is present, LDR ligates the two primers together and generates a fluorescence signal at the appropriate element of the array. Even in the absence of the mutation, the discriminating primers hybridize to their zip code probes but do not generate a fluorescence signature. The challenge in this assay format is that unligated discriminating primer competes with ligated product for a fixed number of hybridization sites. To enhance the signal for this assay format, Gerry and co-workers used gel pads at each element of the array to add a third dimension to increase the loading level of zip code probes.[15] The attractive feature of these universal arrays is that they can be used to detect a variety of different mutations by simply appending the correct zip code complement sequence to the discriminating primer used in the LDR step.

In this paper, we report the development of universal arrays in polymer-based microfluidic chips for the detection of low-abundant mutations. The material of choice for the fluidic device was poly(methyl methacrylate) (PMMA) because we have previously outlined procedures for covalently attaching oligonucleotide probes to the surface of this material and it can readily be micromachined.[47,48] The attractive features of merging microarray technology with microfluidic platforms include the reduced amount of sample required to address each element of the array, the enhanced mass transport to the array surface, which reduces analysis time, the ability to monitor several samples simultaneously using multichannel chips, and the closed architecture of the microfluidic channel reducing the potential for contamination. Several reports have appeared that have discussed microarrays and microfluidics on a single platform. Fan and co-workers used paramagnetic beads as a solid support for the immobilization of target DNA via biotin−streptavidin linkages.[49] A microfluidic device constructed from glass was used to capture the beads magnetically and then interrogate them with fluorescently labeled probes. They were able to demonstrate the hybridization signal reached a maximum in several seconds using pneumatic pumping and the beads containing the target DNA could be interrogated up to 12 times before observing a loss of signal. Benoit et al. developed three-dimensional flow-through arrays in glass chips by fabricating circular channels (10-μm i.d.) that were 0.5−2.0 mm in height.[50] The authors were able to show detection limits for a hybridization assay of 40 pM for the target, which was a 15-mer

(47) Henry, A. C.; Tutt, T. J.; Galloway, M.; Davidson, Y. Y.; McWhorter, C. S.; Soper, S. A.; McCarley, R. L. *Anal. Chem.* **2000**, *72*, 5331−5337.
(48) Waddell, E.; Wang, Y.; Stryjewski, W.; McWhorter, S.; Henry, A. C.; Evans, D.; McCarley, R. L.; Soper, S. A. *Anal. Chem.* **2000**, *72*, 5907−5917.
(49) Fan, Z. H.; Mangru, S.; Granzow, R.; Heaney, P.; Ho, W.; Dong, Q.; Kumar, R. *Anal. Chem.* **1999**, *71*, 4851−4859.
(50) Benoit, V.; Steel, A.; Torres, M.; Lu, Y. Y.; Yang, H. J.; Cooper, J. *Anal. Chem.* **2001**, *73*, 2412−2420.

Table 1. Sequences of Oligonucleotides Used in the LDR and Hybridization Assays

oligos	sequences (5′ → 3′)	T_m (°C)
oligo A	(C6 amino) TTTTTTTTTTTTGTCGTTTTACAACGTCGTG	56.6
M13 FWD (−29) IRD 800	IRD800 C ACG ACG TTG TAA AAC GAC	48.9
zip code 1	TGCGACCTCAGCATCGACCTCAGC-spacer-NH_2[a]	66.4
zip code 3	CAGCACCTGACCATCGATCGCAGC-spacer-NH_2[a]	65.5
zip code 5	GACCACCTTGCGATCGGGTACAGC-spacer-NH_2[a]	66.8
zip code 11	TGCGGGTACAGCACCTACCTTGCG-spacer-NH_2[a]	66.7
Czip11-K-ras c12.2v	**CGCAAGGTAGGTGCTGTACCCGCA**AAACTTGTGGTAGTTGGA GCTG*T*	72.6
K-ras c12 com-2	p[b]TGGCGTAGGCAAGAGTGCCT-IRD 800	69.7

[a] Spacer-NH_2, $PO_4(CH_2CH_2O)_6PO_3(CH_2)_3NH_2$. [b] p, phosphorylated.

labeled with 5′-carboxyfluorescein. Liu and co-workers fabricated a plastic (polycarbonate, PC) chip that integrated PCR and a hybridization array to a monolithic device.[51] The microchips were fabricated using a CO_2 laser and assembled by thermal and adhesive tape bonding. The hybridization probes were tethered to the surface of the PC using a proprietary technique into a chamber that measured 1.2 × 5.0 × 0.25 mm (volume, 7.0 μL). Using a 200-bp PCR-generated product from *Escherichia coli*, they determined that ∼1 h was sufficient for detection of the hybridization event. One potential problem associated with the use of PC is that it generates a significant amount of autofluorescence, which can potentially lower detection limits when fluorescence readouts are used.[52]

In this work, a PCR/LDR assay was carried out on *K-ras* genes to detect the presence of point mutations possessing clinical relevance for diagnosing colorectal cancers. Using presynthesized oligonucleotides, the array containing the zip codes was microprinted into microfluidic channels hot-embossed in PMMA. Following production of the array, the microchip was assembled with a cover plate and the array accessed using microfluidics. The surface chemistry and microfluidic chip was optimized to increase the loading level of the oligonucleotide probes, improve the stability of the linkage chemistry to allow repeated use of the array, increase the kinetic rate of hybridization in the microfluidic channel, and demonstrate high sensitivity (detection of low numbers of mutant DNA in high copy number wild-type DNAs) for this hybridization assay.

EXPERIMENTAL SECTION

Reagents. PMMA used as the universal array and microfluidic chip substrates were purchased from GoodFellow (Berwyn, PA). Chemicals used for PMMA surface modification and hybridization assays included *N*-lithioethylenediamine, ethylenediamine, 50 wt % glutaric dialdehyde, sodium borohydride, sodium cyanoborohydride (5.0 M solution in aqueous ∼1 M sodium hydroxide), perchloric acid, and 20× SSPE buffer, were purchased from Aldrich Chemical (Milwaukee, WI), and were used as received. The sulfo-SDTB reagent for determining the surface concentration of amine groups on PMMA was purchased from Pierce Chemicals (Rockford, IL). Oligonucleotide probes and primers were obtained from three different sources, Midland Certified Reagent Co. (Midland, TX), Li-COR Biotechnology (Lincoln, NE), and IDT (Coralville, IA). Their sequences and melting temperatures (T_m) are listed in Table 1. Ampligase Thermostable DNA ligase was obtained from Epicenter, Inc. (Madison, WI). Typical compositions of solutions used in our experiments were as follows: hybridization solution—10 nM M13 IRD-800 dye-labeled primer, 5× SSPE, and 0.1% SDS; wash buffer—2× SSPE and 0.1% SDS; capping solution—$NaBH_4$ 0.25 g dissolved in 95% ethanol and diluted to 100 mL with 0.1 M phosphate buffer (pH 6.1). All solutions were made in doubly distilled water (18 MΩ·cm) (Barnstead/Thermolyne NANO-pure Infirmity, Dubuque, IA).

Chip Fabrication. Microchips were fabricated using methods previously reported.[53−55] Briefly, the procedure involved fabricating a metal molding die by LIGA, which consisted of raised microstructures electroplated from Ni on a stainless steel base plate (see Figure 2 for picture of molding die). The device topology is depicted in Figure 2. Fluid access channels (DNA sample and wash buffers) were 100 μm in width and 50 μm in depth. Both channels merged into one common channel and emptied into the hybridization chamber, which measured 500 μm in width, 50 μm in depth, and 6.7 mm in length (volume, 168 nL). Replicates from the molding die were hot-embossed into PMMA. The embossing system consisted of a PHI Precision Press model number TS-21-H-C (4A)-5; City of Industry, CA). A vacuum chamber was installed into this press to remove air (pressure <0.1 bar) so complete filling of the die could take place. During embossing, the molding die was heated to 150 °C and pressed into the PMMA wafer with a force of 1 000 lb for 4 min. During this process, the die was heated to 160 °C. After 4 min, the press was opened and the polymer part removed and cooled. The PMMA wafer was maintained at 85 °C throughout the demolding process. The embossed devices were assembled by heat annealing a cover plate made from the same material to the substrate at 105 °C for 2 min. The cover plate and substrate were clamped together and placed in the oven.

Surface Modification. PMMA sheets (6 × 6 mm^2) or the hot-embossed PMMA microchannels were modified (prior to chip assembly) following our previously published procedure, which is schematically illustrated in Scheme 1.[47,48] Briefly, a 0.13 M *N*-lithioethylenediamine solution was prepared by dissolving

(51) Liu, Y.; Rauch, C. B.; Stevens, R. L.; Lenigk, R.; Yang, J.; Rhine, D. B.; Grodzinski, P. *Anal. Chem.* **2002**, *74*, 1170−1177.
(52) Wabuyele, M. B.; Ford, S. M.; Stryjewski, W.; Barrow, J.; Soper, S. A. *Electrophoresis* **2001**, *22*, 3939−3948.
(53) Ford, S. M.; Davies, J.; Kar, B.; Qi, S. D.; McWhorter, S.; Soper, S. A.; Malek, C. K. *J. Biomech. Eng.-Trans. ASME* **1999**, *121*, 13-21.
(54) Galloway, M.; Stryjewski, W.; Henry, A.; Ford, S. M.; Llopis, S.; McCarley, R. L.; Soper, S. A. *Anal. Chem.* **2002**, *74*, 2407−2415.
(55) Ford, S. M.; Kar, B.; McWhorter, S.; Davies, J.; Soper, S. A.; Klopf, M.; Calderon, G.; Saile, V. *J. Microcolumn Sep.* **1998**, *10*, 413−422.

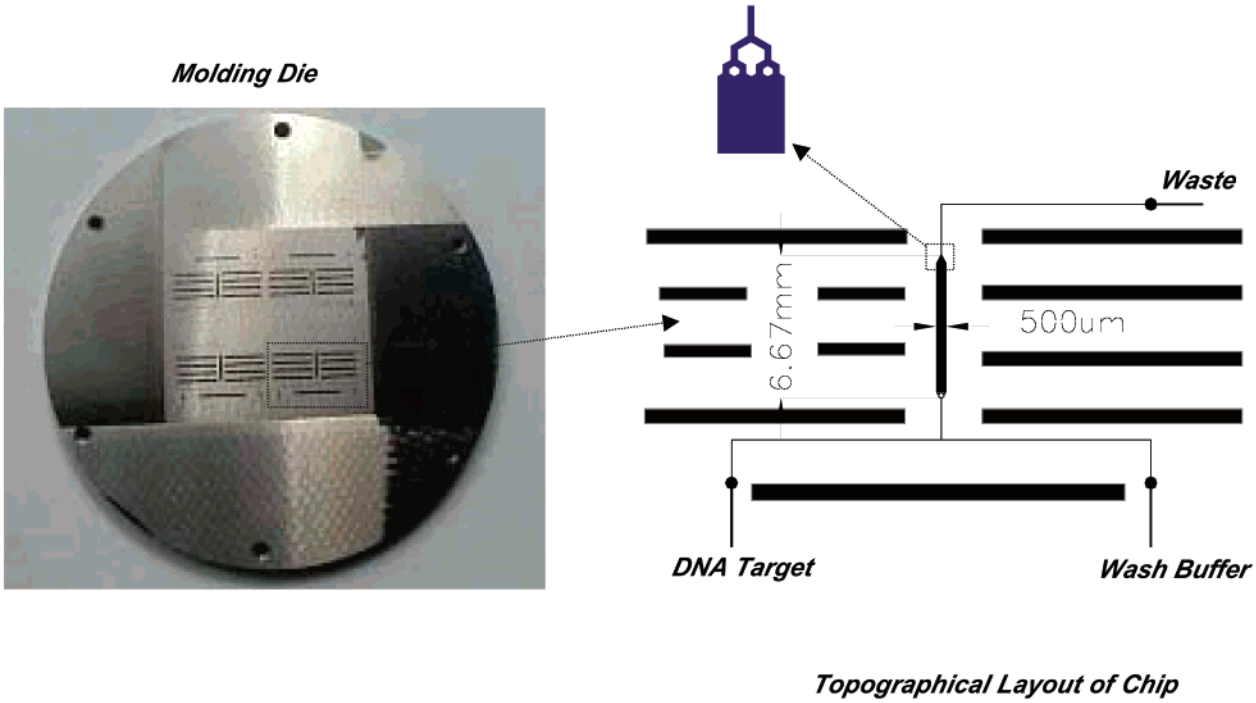

Figure 2. Picture of the Ni molding master fabricated using LIGA and a topographical layout of one of the hybridization microfluidic networks. There are two microchannels for feeding the hybridization chamber: one to deliver the DNA sample to the hybridization chamber and the other, wash buffer. The feed channels were 100 μm in width and 50 μm in depth. The hybridization chamber was 500 μm in width and 50 μm in depth. The chip was hot embossed in PMMA. All dark lines represent raised structures on the molding die. The large horizontal rectangles flanking the fluidic channels were placed on the molding die to assist in bonding of the cover plate to the substrate.

N-lithioethylendiamine in ethylenediamine and magnetically agitating until the solution turned dark purple. PMMA slides were aminated by immersing in the *N*-lithioethylenediamine solution at room temperature. After amination was complete, the slides were thoroughly rinsed with doubly distilled H_2O (ddH_2O). Next, the aminated slides were soaked for 1 h in a 5% glutaric dialdehyde (cross-linking agent) solution containing phosphate buffer (0.5 M, pH 6.4). The 5′-amine-terminated oligonucleotides were then reacted with the activated PMMA surface by spotting the oligonucleotide probes (0.2 μL) on the surface using a micropipettor. Following attachment of the oligonucleotide probes, excess surface aldehydes were capped with sodium borohydride.

A sulfo-SDTB reagent (sulfosuccinimidyl-4,4′-dimethyoxytrityl butyrate) was used to measure the amine surface concentration on the treated PMMA surface. The aminated slides were soaked in 0.1 mM sulfo-SDTB in 50 mM sodium bicarbonate buffer (pH 8.5) at room temperature for 1 h and rinsed thoroughly with ddH_2O. Finally, the slides were dried with compressed air and developed in 1 mL of 35% perchloric acid. The absorbance of the resultant pink solution was measured with a UV−visible spectrometer (Amersham Pharmacia, New York, NY) at 498 nm. The total number of amine groups was calculated from the absorbance value at 498 nm, the extinction coefficient (70 000 cm^{-1} M^{-1}) of the released 4,4′-dimethoxytrityl cation, and the total solution volume (1 mL). The surface amine density for the treated PMMA was then determined by dividing the total amine amount by the surface area (not corrected for roughness). Five samples were included in each measurement, with the average value reported.

Near-IR Laser Scanner. Near-IR fluorescence measurements were made from the arrays with a device built in-house that has been described in a previous publication.[48] Briefly, the near-IR scanner consisted of a diode laser (PicoQuant GmbH, model 800, Berlin, Germany), counting electronics (PicoQuant GmbH, model SPC 430, Berlin, Germany), and a single-photon avalanche diode (SPAD, EG&G Optoelectronics, model SPCM-PQ, Vaudreuil, Canada). The components were mounted with the aid of a mounting cube and lens tubes purchased from ThorLabs (Newton, NJ) and configured in an epi-illumination format. The diode laser operated at a wavelength of 780 nm with 7.5 mW of average power. An integrated optics set was provided with the laser to produce an elliptically shaped collimated output. The laser excitation beam was passed through a 780-nm line filter (Omega Optical, 780DF10, Brattleboro, VT), reflected by a dichroic mirror (Omega Optical, 795DRLP) and focused onto the array surface using a 40× high numerical aperture (NA) microscope objective (Nikon, Natick, MA, NA = 0.85). The $1/e^2$ spot size of the excitation beam was measured to be 3 μm (minor axis) by 5 μm (major axis). The fluorescence excitation was collected by the same microscope objective, transmitted through the dichroic, a circular aperture set at 2.0 mm (clear diameter), and finally through a filter stack consisting of a long-pass filter (cut-on wavelength, 830 nm; Newport Corp., Irvine, CA) and a band-pass filter centered at 825 nm (825RDF30, Omega Optical). After passing through the filters, the fluorescence was sent through a condensing lens (01LAG111/076, Melles Griot) and focused onto a SPAD.

The entire fluorescence detector was mounted on an X/Y microtranslational stage, which was controlled by stepper motors interfaced to a PC computer. Two bipolar stepper motors interfaced to the PC using STP-100 stepper motor controller boards obtained from Pontech, Inc. (Upland, CA) drove the X and Y directions of the microtranslational stages. Each STP-100 was equipped with the RS-485 interface allowing full duplex, multidrop

Scheme 1

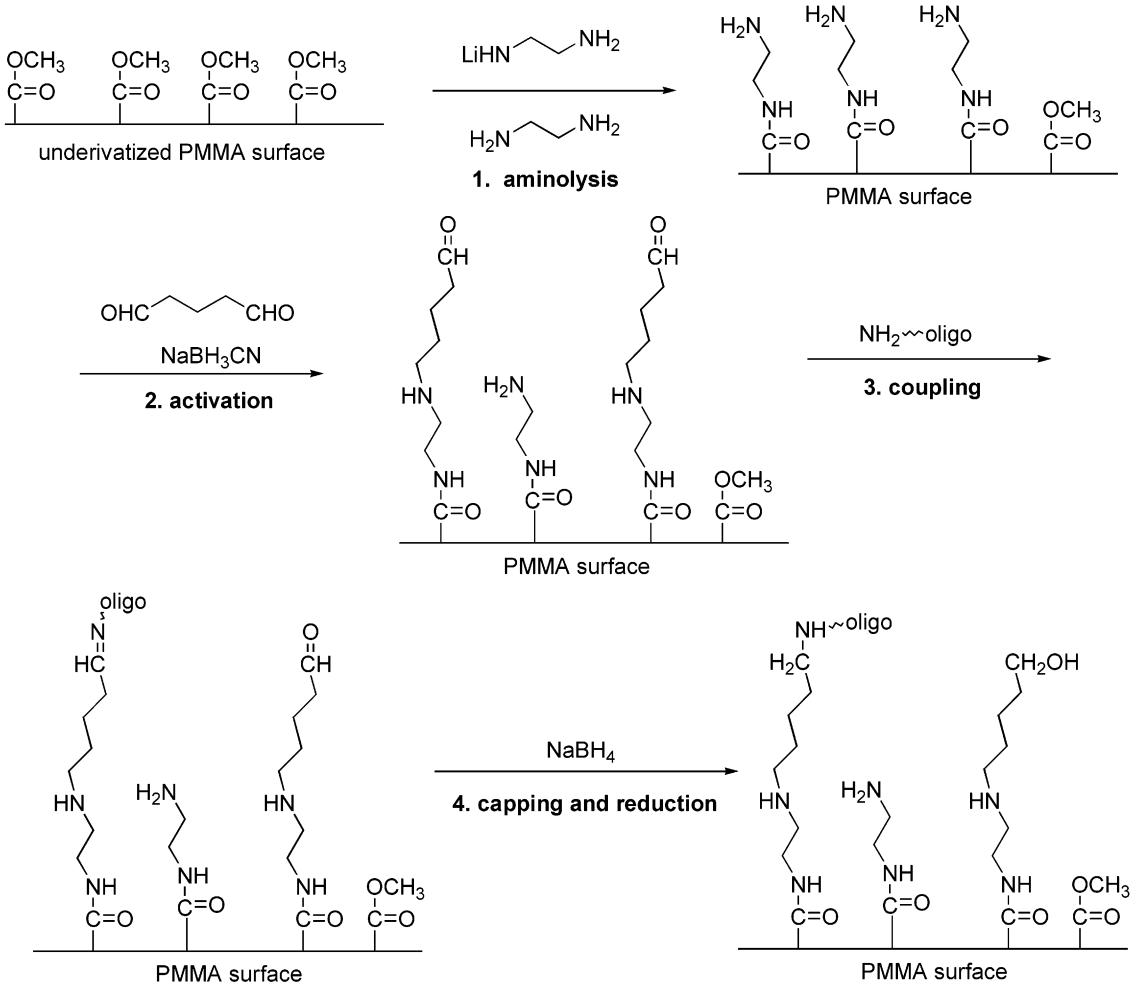

communication with the host computer. A PP232-485f interface (Pontech, Inc.) was used to convert RS485 into the PC's RS232 protocol. Hall sensors were used to monitor the travel limits of the *X*/*Y* stages. The step resolution of these stages was 12.7 μm with a scan range of 4 cm in both the *X* and *Y* coordinates. The scanner operated by taking a single step and then acquiring the fluorescence data for a software-selectable integration period (10 ms−10 s).

The data acquisition software was written in Visual Basic and consisted of several control and data acquisition functions such as recording the position of the scanning head, streaming data to the hard drive, and providing real-time visualization of the acquired images. The size of each data file was determined by the number of pixels included in the image file (set by the stepping resolution and area imaged) with four bytes representing the intensity at each image pixel.

Extraction of DNA from Cell Lines. Genomic DNA was extracted from cell lines of known *K-ras* genotype (HT29, wild type; C12V, mutant).[24] Cell lines were grown in RPMI culture media with 10% bovine serum. Harvested cells ($\sim 1 \times 10^7$) were resuspended in DNA extraction buffer (10 mM Tris-HCl, pH 7.5, 150 mM NaCl, 2 mM EDTA, pH 8.0) containing 0.5% SDS and 200 μg/mL proteinase K and incubated at 37 °C for 4 h. Thirty percent (v/v) of 6 M NaCl was added to the mixture, and the samples were centrifuged. DNA was precipitated from the supernatant with three volumes of EtOH, washed with 70% EtOH, and resuspended in TE buffer (10 mM Tris-HCl, pH 7.2, 2 mM EDTA, pH 8.0).

PCR Amplification of Genomic DNA. PCR amplifications were carried out in 50 μL of 10 mM Tris-HCl buffer (pH 8.3) containing 10 mM KCl, 4.0 mM $MgCl_2$, 250 μM dNTPs, 1 μM forward and reverse primers (50 pmol of each primer), and between 1 and 50 ng of genomic DNA extracted from the cell lines. The primers used were: Ex.1.3 forward = 5′ AAC CTT ATG TGT GAC ATG TTC TAA TAT AGT CAC 3′; Ex.1.4 reverse = 5′ AAA ATG GTC AGA GAA ACC TTT ATC TGT ATC 3′; Ex.2.9 forward = 5′ TCA GGA TTC CTA CAG GAA GCA AGT AGT 3′; and Ex.2.11 reverse = 5′ ATA CAC AAA GAA AGC CCT CCC CA 3′. After a 2-min denaturation step, 1.5 units of Amplitaq DNA polymerase (Perkin-Elmer, Norwalk, CT) was added under hot start conditions and amplification achieved by thermal cycling for 35−40 cycles at 95 °C for 30 s, 60 °C for 30 s, 72 °C for 1 min, and a final extension at 72 °C for 3 min. PCR products were stored at −20 °C until required for the LDR assays.

LDR and Hybridization Conditions. LDRs were executed in a total volume of 80 μL in 0.5-mL polypropylene microtubes. The reaction cocktail consisted of 8 μL of 1 μM c-zip 11 discriminating primer, 8 μL of 1 μM com-2 fluorescently labeled primer (see Table 1 for sequences of primers), 1 μL of 200 mM DTT, 1 μL of 10 mM NAD, and various ratios of mutant (*K-ras*

c12.2v) and wild-type PCR products with the total DNA mass set at 0.1 pmol for each reaction. The concentration ratio of the mutant-to-wild-type DNA was adjusted in the LDR cocktail to 0:1 (mutant/wild type, control) to 1:10 000. The LDR cocktail was taken to a final volume of 80 μL by adding 2× reaction buffer. The LDR mix was then preheated to 94 °C for 2 min followed by the addition of 1 μL of Ampligase enzyme (5000 units/μL, Epicentre). The reaction mix was subjected to 20 LDR thermal cycles using the following temperatures: 94 °C for 30 s; 65 °C for 2 min. To test the fidelity of the LDR reaction, slab gel electrophoresis was run on an aliquot of each reaction (6 μL of reaction mixture mixed with 1 μL of loading dye and 1 μL and then loaded into individual wells of the slab gel). The electrophoresis was accomplished using a cross-linked polyacrylamide gel (8% (w/v), FMC BioProducts, Rockland, ME, with 7 M urea). The gel was polymerized between two borofloat glass plates (21 cm × 47 cm) and placed in an automated DNA sequencer (Li-COR 4000, Li-COR Biotechnology, Lincoln, NE). The electrophoresis was typically run at −1 500 V for 24 h.

Zip code oligonucleotide probes 1, 3, 5, and 11 (see Table 1 for sequences) were dissolved separately in 0.2 M phosphate buffer (pH 8.3) to a final concentration of 0.1 mM. The arrays were microprinted on the activated PMMA using a micropipet. The volume deposited was 0.2 μL of the probe, which resulted in a spot of ∼400 μm in diameter. The spot for each probe was placed along the length of the hybridization chamber. Following deposition of the four probes and capping, the chip was assembled by placing a cover plate over the microfluidic channels, clamping the assembly together and thermally annealing using the procedure described previously. The microchip was then flushed with a rinsing buffer using a syringe pump. The LDR product was pumped through the hybridization chamber at a volumetric flow rate of 1 μL/min with the chip heated to ∼50 °C for 2 min. This was followed by a subsequent wash with the hybridization buffer (2.0 μL/min) for ∼5 min and finally imaging the chamber with the near-IR laser-induced fluorescence scanner.

We could estimate the capture efficiency (CapE) of solution complements in the microfluidic chip from knowledge of the residence time of the complement above its appropriate probe (t), the diffusion coefficient of LDR product (D), the height of the hybridization chamber (h), and the input concentration (C_{in}) using

$$\mathrm{CapE} = \frac{\langle C_{out} \rangle}{C_{in}} = 1 - \frac{[h - \sqrt{2Dt}]}{h} \qquad (1)$$

where $\langle C_{out} \rangle$ is the average output concentration and t is calculated from the linear velocity and the size of the array spot (400 μm). Inserting appropriate values into eq 1 (h = 50 μm; t = 0.61 s; $D = 43 \times 10^{-8}$ cm^2/s)[56] gave a value of 0.14 for CapE using our microchip.

RESULTS AND DISCUSSION

The major focus of our work reported herein was to develop a robust platform for developing arrays appropriate for screening low-abundant mutations in genomic DNA. To this end, several operational characteristics associated with existing microarray platforms were redesigned for the following reasons: (1) to optimize the loading level of DNA probes to the array surface, (2) to improve the stability of the linkage chemistry to allow re-interrogation of the array, (3) to reduce the assay (hybridization) time, (4) high sensitivity in identifying the presence of mutant DNA in high copy number normal DNAs; (5) universal platform for screening a number of different mutations. We decided on developing the arrays using PMMA as the substrate since it can be readily machined to form microfluidic channels using embossing or molding techniques, stable linkage chemistries can be used to immobilize probes,[47,48] and the autofluorescence generated from this polymer material is low when interrogated with near-IR fluorescence.[52]

Optimization of Coupling Chemistry to PMMA Substrate. A protocol that permits end attachment of amine-terminated oligonucleotides to a PMMA surface is shown in Scheme 1.[47] In our previous work using arrays assembled onto sheet PMMA surfaces, the surface loading level of probe was not optimized. Because it is anticipated that the surface amine groups serve as initial sites for oligonucleotide attachment as shown in Scheme 1, their surface density should be crucial to provide a sufficient number of capture sites for a minority of ligated zip code complements. Thus, the amine surface density was measured as a function of amination time to provide an optimized number of tethering sites. As shown in Figure 3, the amine density increased initially with amination time up to ∼180 min and then saturated at a surface concentration of (7.68 ± 0.5) × 10^{-9} mol/cm^2. This surface concentration of amines is higher than the silanol density found on glass by nearly 1 order of magnitude.[41] We suspect that the modification chemistry is not limited to activation of only surface exposed groups, but underlying layers of the polymer as well, which provides an *apparent* higher concentration of surface amine groups compared to glass.[47]

Increasing the number of functional amine sites on the PMMA may not necessarily result in increased loading of complements on the surface following hybridization due to steric considerations or a higher hybridization signal when using fluorescence readout.[41] Therefore, we carried out experiments in which oligonucleotide probes were tethered to sheet PMMA and an IRD800-labeled oligonucleotide complement hybridized to the array as a function of the amination time. The results of this study are shown in Figure 3. As can be seen, the fluorescence intensity did not show a direct correlation with amination time (and therefore, surface amine density). Instead, the intensity decreased monotonically with amination time in the first 60 min and subsequently plateaued. As the amination time increased from 5 to 180 min, the amine surface density increased by 2.5-fold whereas the fluorescence intensity decreased by 4.5-fold. Two reasons may be responsible for these observations: (1) self-quenching of fluorophores as they are brought into close proximity on the surface;[57] (2) steric hindrance of surface-bound oligonucleotide probes at higher surface densities.[39] In addition to the observed fluorescence changes, longer amination times (>60 min) led to a roughening of the PMMA surface and a transition from transparent to an opaque PMMA surface due to slight dissolution of the PMMA by

(56) Stellwagen, N. C.; Magnusdottir, S.; Gelfi, C.; Righetti, P. G. *Biopolymers* **2001**, *58*, 390−397.

(57) Shchepinov, M. S. C.-G.; Southern, E. M. *Nucleic Acids Res.* **1997**, *25*, 1155−1161.

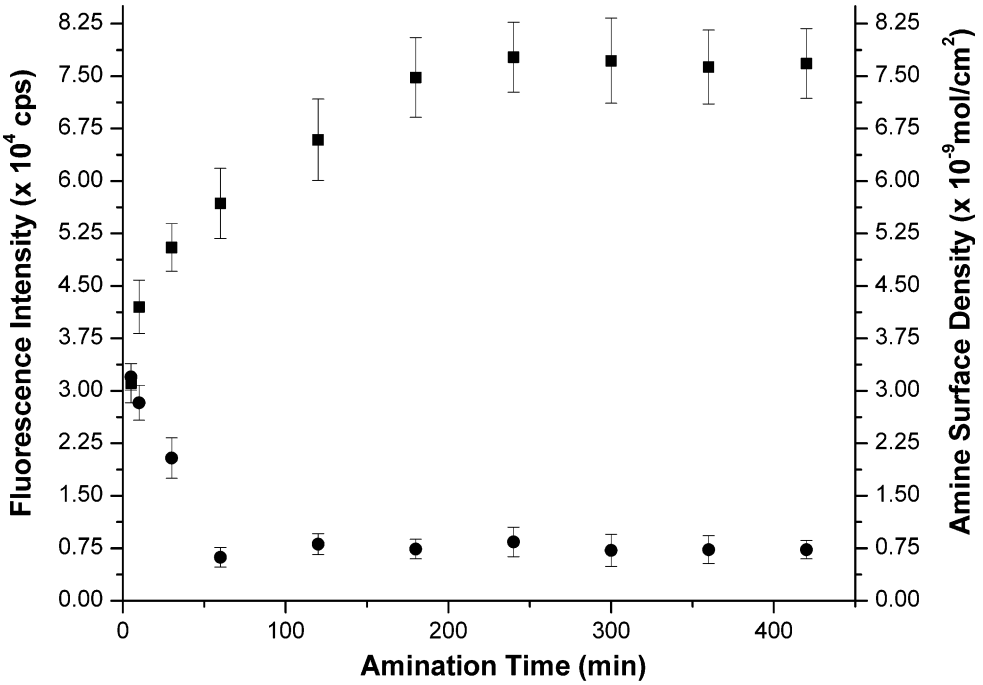

Figure 3. Surface amine density (squares) and fluorescence intensity (circles) of the hybridization signal as a function of amination time. The surface amine concentration was determined using the sulfo-SDTB reagent (see Experimental Section). Sheet PMMA squares (6 × 6 mm^2) were aminated in 0.13 M *N*-lithioethylenediamine solution at room temperature for a series of times ranging from 5 min to 7 h. Five slides were included in each time group with the average value shown. The error bars represent the standard deviation in the measurement series. The immobilized probes were complements (19-mer) to an M13-IRD 800-labeled oligonucleotide. The fluorescence was acquired using a near-IR confocal scanning imager.

the modification solvent. Therefore, short amination times (in the range of 15−30 min) were chosen to modify the PMMA surface, which resulted in maximum fluorescence signals following hybridization.

Stability of Linkage Chemistry. For the zip code microarray, the array could be used to screen for a number of different mutations in different assays by appending the appropriate zip code complement to the ligation primer. Therefore, reusability of the constructed microarray is desirable. We used arrays spotted on PMMA sheets to examine the stability of the linkage chemistry toward typical denaturing conditions. The DNA duplexes on the surface carrying a fluorescent label were denatured and rehybridized, and the fluorescence intensity was examined after each cycle. The hybridized PMMA slides were denatured in 1:1 formamide/NaOH (0.5%) at 95 °C for ∼10 min. After each denaturation step, the slide was scanned to examine for the absence of fluorescence on the surface. Two different linkage chemistries were investigated, an imine bond between the amine and surface-tethered aldehyde and the resultant secondary amine formed after reduction of the imine linkage. We found that, after two cycles of denaturation/hybridization, the imine linkage produced hybridization signals that were reduced to ∼5% of their original intensities (data not shown). However, when the imine linkage was reduced to a secondary amine, the PMMA-based arrays did not show appreciable degradation of signal even after 12 cycles (see Figure 4). This result was attributed to the selective reduction by sodium cyanoborohydride of the imine bond. The sodium cyanoborohydride converts the less stable imine bond to a more stable secondary amine. When the oligonucleotide slides were capped in sodium borohydride, residual aldehyde groups were transformed to primary alcohols and also the imine bonds between the zip code oligonucleotides and the cross-linker were reduced (see Scheme 1). We noticed that, following capping using sodium

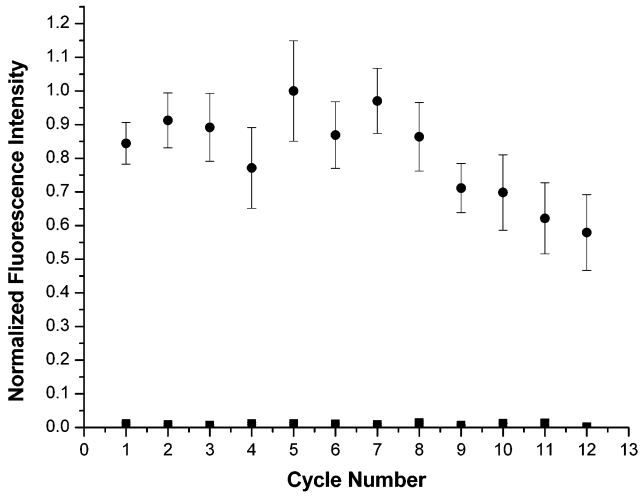

Figure 4. Stability of the oligonucleotide−PMMA coupling chemistry as a function of denaturation/hybridization cycles. The average hybridization fluorescence intensity (circles) from five different spots of an array is shown. The aminated PMMA slides were soaked in 5% glutaric dialdehyde solution with 10 μL/mL sodium cyanoborohydride added and the capping step finished in $NaBH_4$ for 15 min. Between each hybridization step, the denatured slides were imaged with the fluorescence scanner (squares) to ensure that all labeled oligonucleotide had been removed from the slide. Denaturation was carried out by heating the slide to 95 °C in formamide/NaOH (0.5%) for ∼10 min. The probes were complements to the M13-IRD 800-labeled oligonucleotide.

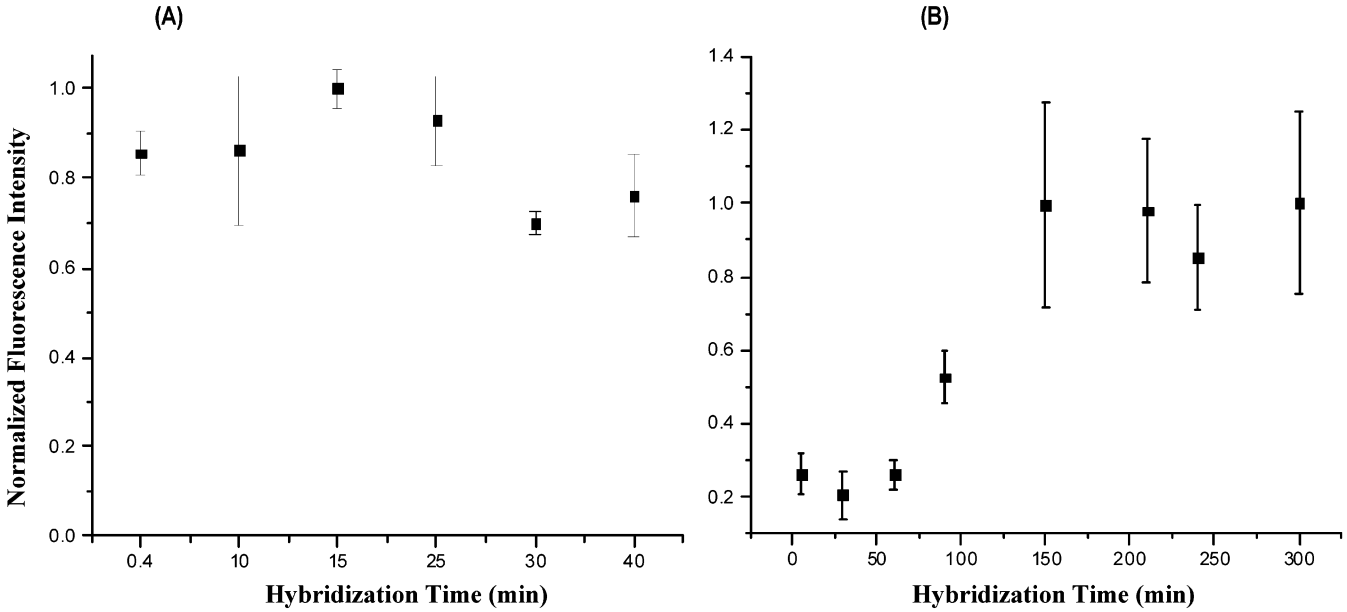

Figure 5. Hybridization kinetics on PMMA microchip channels (A) and sheet PMMA slides (B). PMMA slides were soaked in the hybridization solution at 37 °C for different lengths of time ranging from 5 min to 5 h. For the microchannel assays, the hybridization solution was pushed through the chip using a syringe pump at a volume flow rate of 1 μL/min. After a fixed incubation time, the chip was briefly rinsed with a wash buffer and imaged using the near-IR scanner with the average fluorescence intensity extracted from each spot of the array. The tethered probes were complements to the M13-IRD800-labeled oligonucleotide.

borohydride to produce the alcohol of the reactive aldehyde, very little nonspecific adsorption of solution complement to the surface was also observed. This should result in improved imaging and signal-to-noise ratio in the readout phase of the assay.

Hybridization Characteristics in PMMA Microfluidic Chips. Hybridization assays were then performed in hot-embossed PMMA microfluidic channels and compared to hybridization signals obtained from PMMA slides. Figure 5A shows the normalized fluorescence intensities obtained from four oligonucleotide spots in the fluidic channel with hybridization incubation times ranging from 24 s to 40 min. The data suggested that the fluorescence intensity saturated at or before our first data point in the microfluidic format and remained nearly constant for longer hybridization times. As a comparison, Figure 5B shows the normalized fluorescence intensities acquired from four hybridization assays carried out on PMMA slides with hybridization times ranging from 5 min to 5 h. In this format, the time required for the fluorescence intensity to saturate is much longer (~3 h). The forced flow of target solution over the probe-tethered surface provides enhanced mass transfer of targets to the surface-immobilized probes reducing hybridization time. In addition, the small volume of the hybridization chamber reduces the diffusional distances required for target to reach the surface probes.

An additional advantage associated with the PMMA microfluidic arrays is that the required assembly temperature is much lower than that required for glass.[58] Therefore, the oligonucleotide probes can be coupled to the surface prior to chip assembly provided that the probes do not suffer from chemical degradation during heat annealing. We found no appreciable differences between the fluorescence signal generated from arrays situated in microfluidic chips and those placed on planar PMMA surfaces, indicating little if any chemical degradation of the spotted probes during device assembly (data not shown).

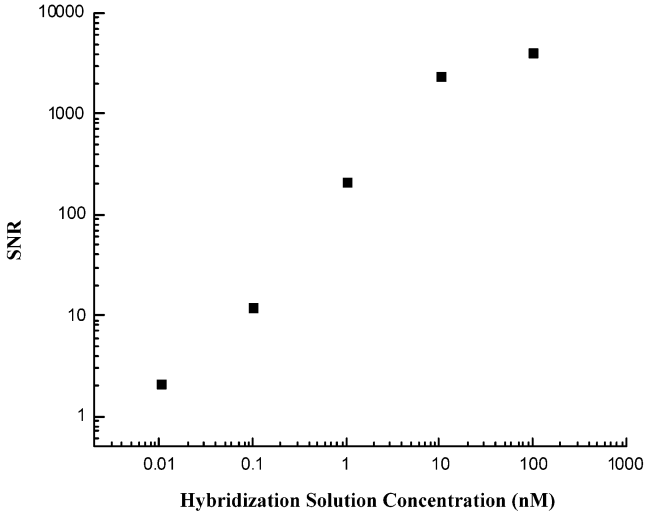

Figure 6. Fluorescence intensity versus concentration of dye-labeled oligonucleotides in the hybridization solution. Each assay was hybridized in different concentrations of the complement (M13-IRD 800 oligonucleotide) at 37 °C. The arrays were scanned with the near-IR scanner and the fluorescence intensity extracted from each spot with the average values plotted for each concentration value.

Figure 6 shows near-IR detection sensitivities in a logarithmic scale at various concentrations of M13-IRD800 labeled primer hybridized to its surface-tethered complement. The arrays were hybridized in 10 pM−100 nM solutions at 37 °C for 30 min. The integration time of the scanner was set at 0.1 s/pixel. As can be seen from this figure, the logarithmic scale of signal-to-noise ratio (SNR, defined as (signal − background)/(background)$^{1/2}$) increased linearly with concentration up to ~10 nM and tended to saturate above that due to the limited number of capture sites. At

(58) Reyes, D. R. I., D.; Auroux, P. A.; Manz, A. *Anal. Chem.* **2002**, *74*, 2623−2652.

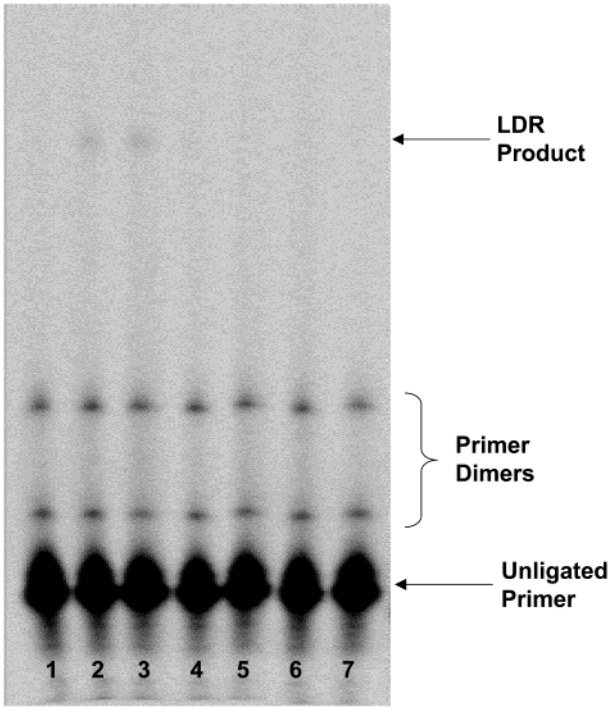

Figure 7. LDR reactions of *K-ras* C12.1V mutant and C12 wild-type DNAs with different ratios of mutant to wild type. Lane 1, control (no mutant); lane 2, 1:1 (mutant/wild type); lane 3, 1:20; lane 4, 1:100; lane 5, 1:1000; lane 6, 1:10 000; lane 7, control. The PCR-amplified genomic DNA was denatured at 94 °C for 2 min, and 1 μL ampligase (5000 unit/μL) was added. The LDR reaction consisted of 20 thermal cycles at 94 °C for 30 s and 65 °C for 2 min. Two microliters of loading buffer and 1 μL of the LDR product were mixed and then 1 μL of this mixture was loaded into an 8% denaturing gel and run on the LICOR DNA sequencer.

the lowest concentration investigated (10 pM), we observed a SNR of 2.05 ± 0.28.

Detecting *K-ras* Mutations Using PMMA Microfluidic Arrays. As a demonstration of the use of these microfluidic arrays for the detection of low-abundant point mutations, 24-mer zip codes were spotted into hot-embossed PMMA microfluidic channels. An LDR was used to generate fluorescent ligation products containing the zip code complement. The LDRs were carried out in a series of solutions consisting of c-zip 11 *K-ras* c12.2v (discriminating primer has sequence complementary to zip code 11 at its 5′-end and the nucleotide complementary to one of the possible point mutations at it 3′-end), *K-ras* c12 com-2 (common primer containing fluorescent label at its 3′-end and phosphorylated base at its 5′-end), the *K-ras* c12.2 v mutant and wild-type PCR products. When the ligated dye-labeled LDR product and unligated discriminating primer was pumped through the channel it was captured by the appropriate zip code. The uncaptured product was removed by flushing with a washing buffer. The fluorescent signal detected at a specific zip code indicates the presence of the corresponding mutation in the examined sample.

Figure 7 shows a slab gel image of the LDR products taken from a DNA sequencer using fluorescence detection. As can be seen in the control lane, only the com-2 primer was detected without LDR product present in that lane. The LDR product could be detected at mutant.wild-type ratios of 1:1 and 1:20 but were not visible in the gel tracks at lower ratios of mutant/wild-type DNA. The LDR product was not visible at these lower ratios due to the low amount of LDR product generated.

We next interrogated the 1:10 000 mutant/wild-type LDR reaction using the PMMA microfluidic device, which contained zip codes 1, 3, 5, and 11. As can be seen from the image displayed in Figure 8, a very intense signal appeared on zip code 11, which is the appropriate zip code for this particular mutation. We also ran a control experiment, in which no mutant DNA was present in the LDR, and found no observable hybridization signal using zip codes 1, 3, 5, and 11 printed into one channel of the microfluidic chip (data not shown). Therefore, despite a large excess of wild-type DNA with a small amount of ligation product, the mutation could be detected. The hybridization of LDR products in the microchannel was conducted at 50 °C, which is 15 °C lower than the melting temperature of the zip codes and should be optimum for hybridization stringency, since mismatches would have a considerably lower T_m.[59] The number of ligated products captured at the appropriate spot of the array is hard to estimate, but the upper limit can be determined from the surface concentration of functional amine sites at the optimized amination time (3.4×10^{-9} mol/cm^2), the ratio of mutant to wild-type sequences (1:10 000), the number of LDR thermal cycles (40), and the capture efficiency (amount of solution complements reaching the surface, CapE = 0.14). Using these values, we estimated 7.9×10^{-13} mol/cm^2 dye molecules detected in the assay. If the spot on the array was 400 μm in diameter, then the mass of dye comprising this signal would be 1.0 fmol if all potential sites were occupied. This hybridization signal was produced from a LDR solution with an approximate concentration of ligated products (hybridization solution) equal to 400 pM, well above our concentration detection limit for this hybridization assay (see Figure 6). The high sensitivity is due in part to enhanced rates of complement capture produced by the microfluidic format, the low levels of nonspecific adsorption of DNA to the functionalized polymer surface, and the use of near-IR fluorescence, which results in low background levels generated from the array substrate and reagents used in the assay.[48,60] As can be seen from eq 1, the shallow height of the hybridization chamber was also critical to provide a high capture efficiency for low-concentration targets.

CONCLUSIONS

We have successfully demonstrated the ability to detect point mutations in certain gene fragments using universal zip code arrays placed into PMMA microfluidic channels fabricated using hot embossing. Our experiments indicated the ability to detect one mutant DNA in 10 000 normal sequences. The coupling chemistry in the PMMA channel was optimized to provide high loading of amine functional groups, optimized fluorescence signal generated following hybridization, and favorable linkage chemistry stability to allow re-interrogation of the array. The linkage chemistry consisted of the use of a dialdehyde bifunctional linker, forming an imine bond between the surface aldehyde and the amine-terminated oligonucleotide probe, which was subsequently reduced to a secondary amine. The hybridization kinetics using this microchip was compared to a planar surface array. The zip code arrays constructed in microfluidic channels were found to

(59) Brown, T. A. *Molecular Biology*; Academic Press: New York, 1998.
(60) Williams, D. C.; Soper, S. A. *Anal. Chem.* **1995**, *67*, 3427−3432.

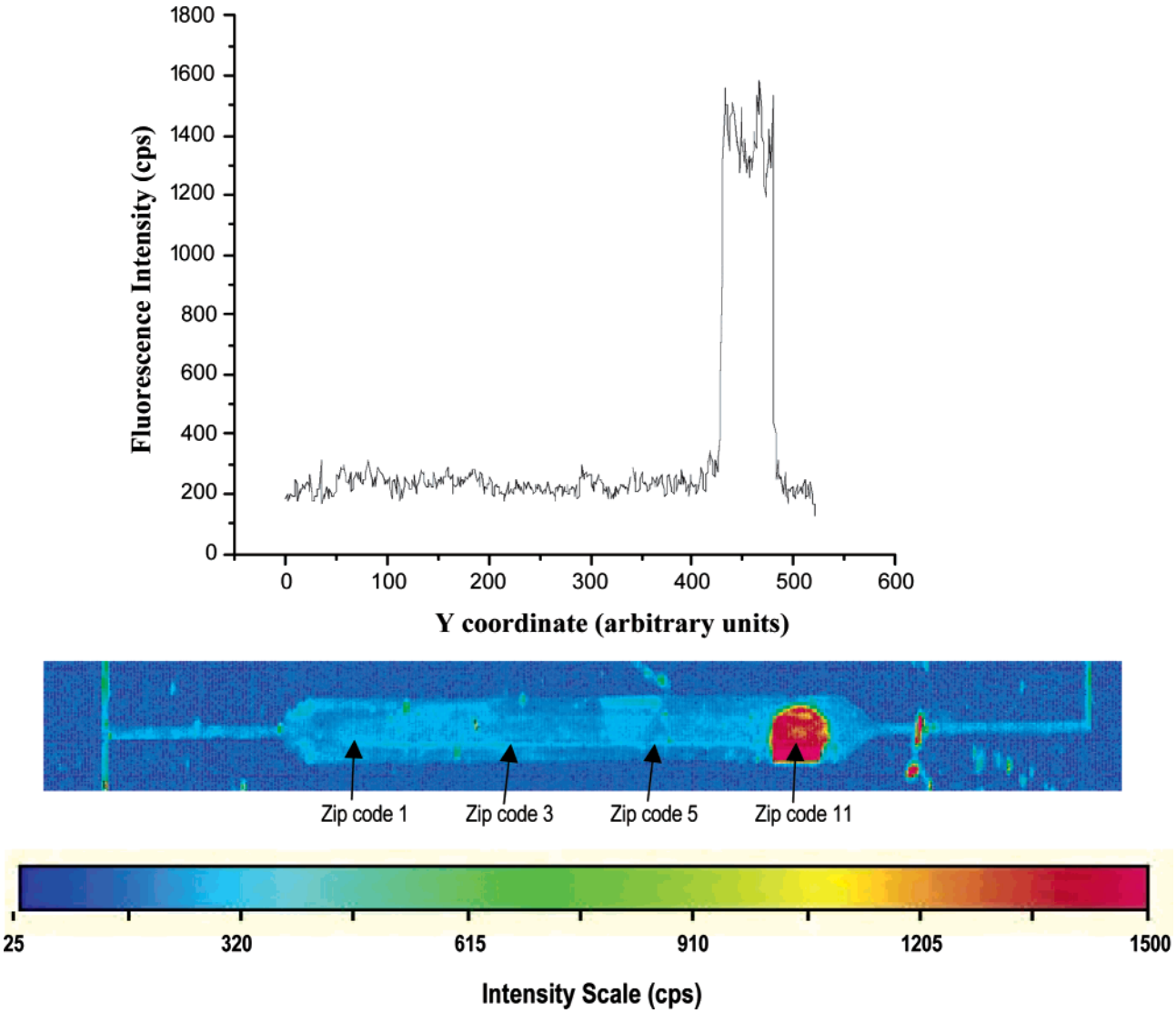

Figure 8. Mutational analysis of 1:10 000 C12.1 mutant-to-wild-type LDR products using the zip code PMMA microchip array. The hybridization solution was pumped through the chip using a syringe pump at a flow rate of 1 μL/min (50 °C hybridization temperature). The chip was scanned using the near-IR scanner. The top trace is a line scan through the center of the microchannel image.

display enhanced hybridization kinetics compared to the planar format due to enhanced mass transfer to the PMMA surface. In addition, the low-temperature assembly required for the device allowed prespotting the probes into an open channel format and then assembling the cover plate to the device with no noticeable degradation in hybridization signal. This format will allow the use of conventional spotting machines to construct the arrays in the microchannels and then accessing the arrays using microfluidics. The universal array format adopted here using zip code capture elements can serve as a viable platform for detecting a number of different mutations in different gene fragments due to the high stability of the linkage chemistry and the ability to effectively remove hybridized complements from the surface.

ACKNOWLEDGMENT

The authors thank the National Institutes of Health (NCI/NHGRI, R24-CA84625) for financial support of this work. Appreciation is also expressed to Dr. Shize Qi for the fabrication of the molding tool and to Mr. James Barrow for hot embossing the final parts. The authors also thank the Center for Advanced Microstructures and Devices (CAMD) at LSU for their assistance in performing the X-ray LIGA.

Received for review November 5, 2002. Accepted December 12, 2002.

AC020683W